Colloid Polym Sci (2009) 287:487–493
DOI 10.1007/s00396-008-1989-5

SHORT COMMUNICATION

Conductive composites based on core–shell polyaniline nanoclay by latex blending

Yingfeng Yu · Xinhui Zhong · Wenjun Gan

Received: 25 November 2008 / Revised: 10 December 2008 / Accepted: 15 December 2008 / Published online: 9 January 2009

Abstract A simple and versatile method for the preparation of conductive composites based on core–shell polyaniline (PANI) one-dimensional nanoclay distributed in poly(ethylene-vinyl acetate) (EVA) latex with high colloidal stability is demonstrated. The morphological and electrical properties of the composites were investigated. The nanostructures were synthesized from PANI-coated sepiolite nanorods via in situ oxidative polymerization after the surface modification of the sepiolite with ammonium and anilinium salts. Two forms of PANI nanoclay, powder and paste, have shown a much different percolation threshold and significantly different morphologies due to their dispersion ability in EVA matrix. At the same PANI content, the conductivity of the blends with paste is much higher than that of blends with powder PANI nanoclay.

Keywords Conducting polymers · Nanocomposites · Polyaniline · Blending

Introduction

It is widely accepted that the conductivity of insulating polymers with conductive fillers is a result of the development of a network of touching filler particles. Many percolation models have been developed to define the critical filler volume fraction, at which a network is formed in conductive polymer compounds. The most prominent one was created by Kirkpatrick [1] and Zallen [2], in which the required minimum filler volume fraction to form a continuous network of touching particles is 16 vol.%.

For years, further studies have shown that the key factors to achieve high conductivity in polymer-based composites are primarily the conductivity and dimension of fillers, followed by the filler dispersion, i.e., an effective filler dispersion to achieve high conductivity [3–5]. For example, depending on carbon nanotubes (CNT) quality, conductivity, dimension, and dispersion, the percolation threshold of CNT in polymers was varied from CNT volume fraction 0.1 vol.% to 10 wt.% [6–8].

Recently, various nanoscale applications, e.g., low percolation threshold of conductivity, have motivated the synthesis of one-dimensional conducting nanomaterials such as nanofibers, nanotubes, and nanorods [9]. The template polymerization of conducting polymers is one of the most facile ways to obtain nanoscaled materials [10–13]. One-dimensional polyaniline (PANI) nanotubes/fibers were well prepared with different templates, such as metal oxide [14, 15], gold and other metals [16, 17], CNTs [18–21], and other nanomaterials [22–25].

For instance, Sainz et al. [18] polymerized PANI onto CNT resulting in a soluble CNT/PANI composite that displayed higher thermal and electrical properties. The thickness of the PANI layer on CNT could be conveniently tuned by the feeding amount of the monomer and polymerization con-

---

Y. Yu (✉) · X. Zhong
Key Laboratory of Molecular Engineering of
Polymers of the Ministry of Education,
Department of Macromolecular Science, Fudan University,
Shanghai 200433, China
e-mail: yfyu@fudan.edu.cn

Y. Yu
Departament de Química Analítica i Química Orgànica,
Universitat Rovira i Virgili,
Macel.li Domingo s/n,
43007 Tarragona, Spain

W. Gan
Department of Macromolecular Materials and Engineering,
College of Chemistry and Chemical Engineering,
Shanghai University of Engineering Science,
Shanghai 200065, China

ditions [26, 27]. Moreover, the high aspect ratio of PANI/single-wall CNT enables percolation into a conducting network at extremely low nanotube concentrations [28].

In other cases, Yu et al. synthesized uniform PANI-sodium alginate nanofibers template-guided by alginate. The biopolymer-PANI nanofibers with uniform diameters varying from 40 to 100 nm were obtained by changing the ratio of aniline to alginate [29].

However, to well disperse these nanoconducting particles into polymer matrix is one of the most difficult challenges for high-conducting composites. Well dispersion of nanopartilces was achieved either by high affinity or by good miscibility in the following cases. Hu et al. [30] prepared binary conductive polymer composites with percolation thresholds as low as 0.2 vol.% through blending carbon black and polyurethane latex.

For PANI, Goh et al. [31] had found that poly(vinyl acetate) (PVAc) can be miscible with *p*-phenolsulfonic acid-doped PANI. Blends containing 50 wt.% or less of PANI-PSA were miscible with PVAc. Barra et al. [32] also studied the conducting blends of ethylene-vinyl acetate (EVA) copolymers and PANI doped with dodecylbenzenesulfonic acid (DBSA). The percolation threshold point and morphology were closely related to methods of polymerization and blending.

With these in mind, in this article, we first prepared PANI nanorods with one-dimensional natural clay, sepiolite, as templates, then chose poly EVA latex to disperse the nanoparticles (as shown in Scheme 1) based on the following two reasons: the high affinity of doped PANI to water with surfactants (latex) and the good miscibility of PANI to PVAc. The resultant conducting materials show a low percolation threshold and high colloidal stability due to the well dispersion of nanoparticles.

Experimental

Materials

Sepiolite nanoclay was provided by Tolsa, Madrid, Spain, as a fine white powder. Poly(vinyl acetate-ethylene) (EVA, Celvolit® 1602) aqueous latex (55 wt.% solid content, Tg=12 °C) was supplied by Celvolit. Aniline (Sinopharm Chemical Reagent, Shanghai, China) was freshly distilled under pressure before use. Concentrated hydrochloric acid, dimethyl dioctadecylammonium bromide (DODAB), ammonium persulfate (APS), and DBSA were received from Sinopharm Chemical Reagent and used without further purification.

Polymerization and blending

The nanoscaled sepiolite was pretreated with the ammonium salt DODAB in a flask under magnetic stirring as follows: DODAB (0.2 g) was added into 300 ml water and 2.0 g sepiolite was dispersed into the mixture in ultrasonic bath for 2 h. Then, different weight ratios of aniline and DBSA (at a stoichiometric ratio) to sepiolite were added into the suspension, the mixture was stirred for 12 h under magnetic stirring, and the suspension was redispersed in ultrasonic bath for another 2 h. The above prepared homogenous milky dispersion was cooled (0 °C) with mechanical stirring in an ultrasonic bath, and a solution of APS oxidant was added dropwise to initiate polymerization. The polymerization reaction was stopped after the dispersion became dark green, indicative of the formation of emeraldine salt with nanoclay. The stable dispersion, containing PANI–DBSA-clay particles, excess DBSA, DODAB, and water, was subsequently treated by two different ways. The first method was to add methanol to the dispersion in order to precipitate the doped PANI composites. The precipitate was filtered, washed with deionized water, and dried under vacuum at 60 °C overnight. The dry product was pulverized into fine powder. The second method was to concentrate the dispersion by filtering the product, at the same time washing it with deionized water for several times until the pH value changed to 7. The resultant product is a dark-green, paste-like PANI–DBSA-clay dispersion (about 10 wt.% concentration).

The PANI nanoclay, either in paste or in powder state, was blended with EVA latex directly by mechanical stirring at 200 rpm for 2 h. For the powder form of PANI nanoclay, another 2 h of dispersion in an ultrasonic bath was

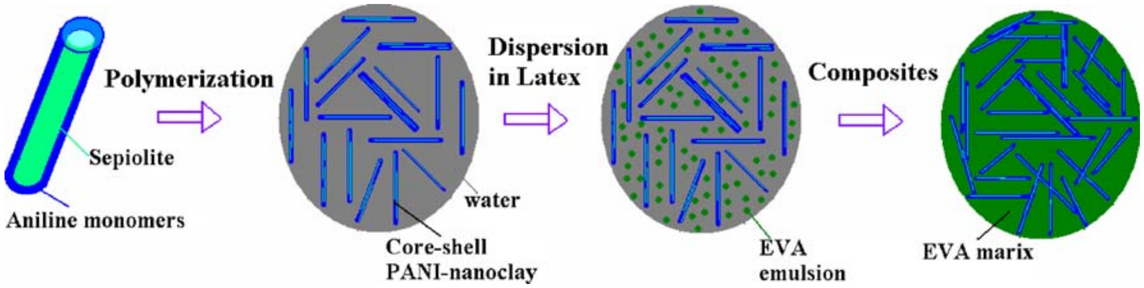

Scheme 1 Schematic representation of template polymerization of PANI on sepiolite and the formation of conductive nanocomposites via latex blending

performed. The resultant green mixture was sealed and preserved at room temperature.

Characterization

For transmission electron microscopy (TEM) study of the structure of sepiolite, a drop of diluted (0.01 wt.%) DODAB-treated clay in water was put on the carbon-coated copper grids, the water was evaporated, and the samples were imaged at 12-kV accelerating voltage by a TEM-100CX apparatus, manufactured by JEOL, Tokyo, Japan. The structures of PANI nanoclay and their blends with EVA latex were observed under a scanning electron microscope (SEM) (Tescan TS 5163 MM) at 20-kV accelerating voltage. The samples were observed directly without coating them with a gold layer due to their high conductivity. Infrared spectra were recorded on a Nicolet NEXUS 470 Fourier transform infrared spectrometer using samples in KBr pellets. X-ray diffraction experiments were performed with a Philips (Andover, MA, USA) X'pert MPD Pro X-ray diffractometer. Thermal decompositions were performed from room temperature to 700 °C on powdered samples with masses between 8 and 15 mg using a Mettler-Toledo TGA-50 thermogravimetric analyzer at a

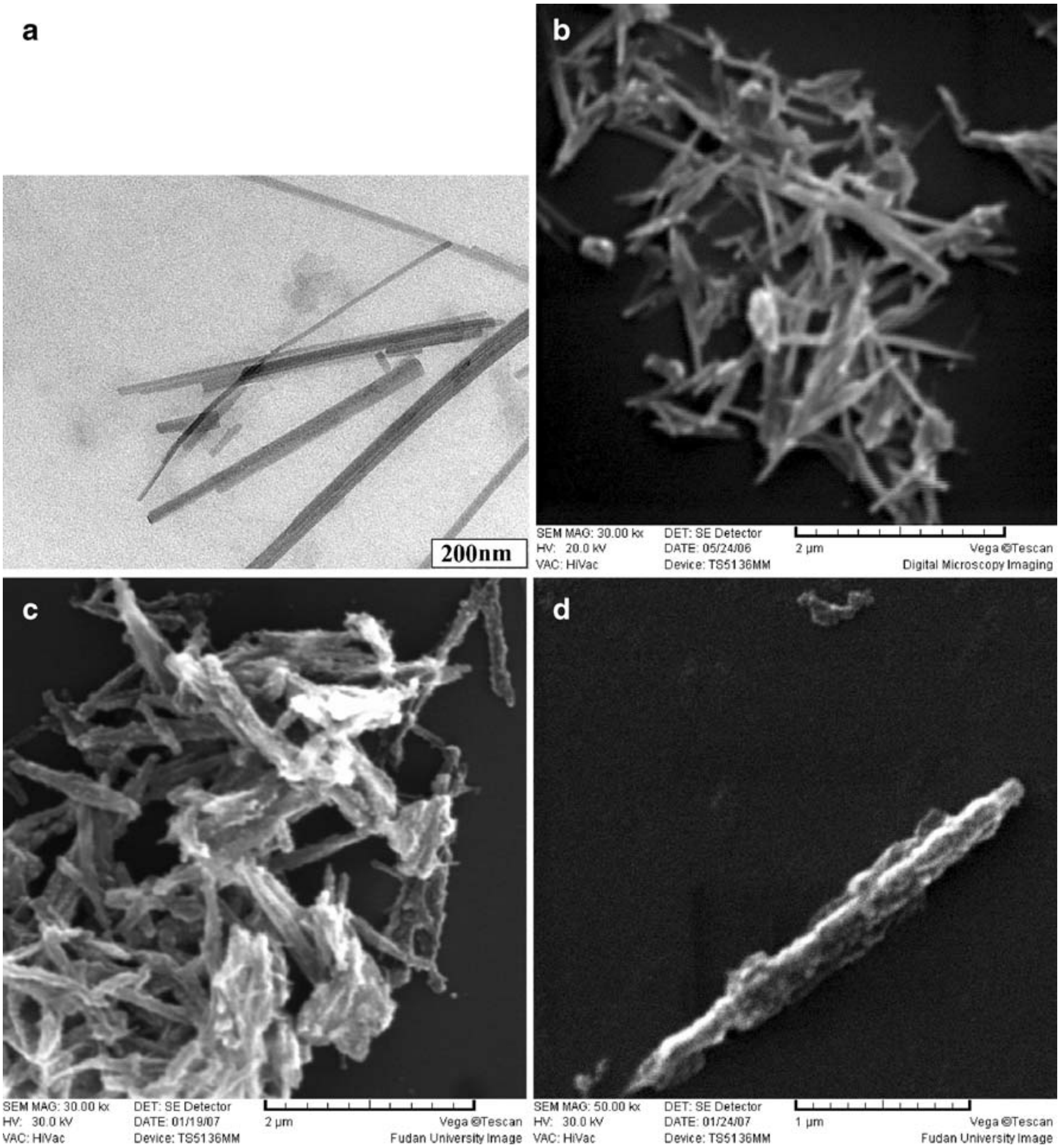

Fig. 1 Morphologies of sepiolite and PANI nanoclay. **a** TEM imagine of sepiolite in water; **b** SEM image of PANI nanoclay with aniline/DSBA–sepiolite = 1:3; **c** SEM image of PANI nanoclay with aniline/DSBA–sepiolite = 2:1; **d** magnification of the rod-like PANI nanoclay

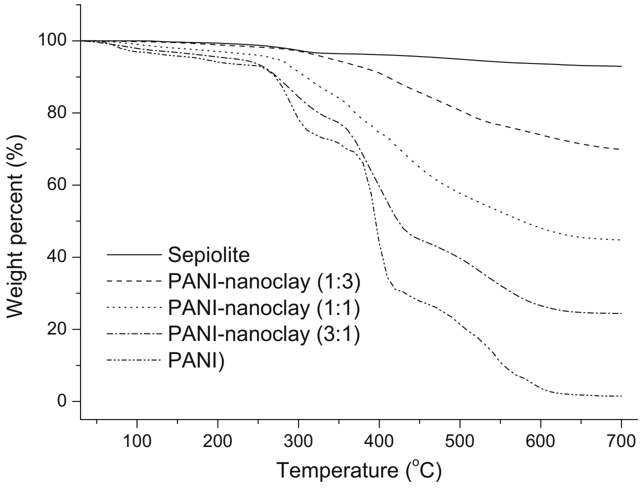

Fig. 2 TGA thermograms of sepiolite and PANI in different ratios

heating rate of 10 °C/min in a nitrogen atmosphere. The electrical conductivity of films (up to 10^{-7} S/cm) was measured using the “four-probe technique” (ASTM D 991-89). The electrical conductivity of less conductive films was measured using the “two-electrode technique” (DIN 53596). Samples for the latter technique were coated with a silver paint to reduce the sample–electrode contact resistance.

Results and discussion

Sepiolite is a type of natural fibrillar silicate clay, and its fibrillar single crystal is the smallest structure unit with a length of 500–2,000 nm and a diameter of 10–25 nm. As shown in Fig. 1a, in a good solvent, such as water, the grafted ammonium salt and surfactant layer acts as a steric stabilizer that gives the particle steeply repulsive interactions. As a result, individual rod-like clay particles could be observed in the TEM images; however, the particle has larger specific surface area, so that aggregated particles of two or three rods together were also found.

For the preparation of core–shell PANI nanoclay, the weight ratio of aniline/DBSA to sepiolite was varied from 1:3 to 3:1 during synthesis. The similar infrared spectrum of neat PANI/DBSA and PANI nanoclay with different ratios of sepiolite demonstrated the well polymerization of aniline with sepiolite. Two absorption bands at 1,585 and 1,498 cm^{-1} were observed corresponding to quinoid and benzenoid ring deformations, respectively, which is in good agreement with the characteristic bands of emeraldine salt reported in the literature [33]. The C–N stretching of the secondary aromatic amine and aromatic C–H out-of-plane bending modes are also observed at 1,305 and 829 cm^{-1}, respectively. TGA curves of the neat sepiolite, PANI, and PANI nanoclay composite particles prepared with different ratios of sepiolite correspond well with IR results (as shown in Fig. 2).

With the increase in weight percentage of aniline/DBSA, the conductivity of the resultant PANI-coated sepiolite is found to increase from 0.02 S/cm for aniline/DBSA to sepiolite=1:3 to 0.1 S/cm for aniline/DBSA to sepiolite= 1:2, and it almost attains the maximum value of 0.2 S/cm when the weight ratio of aniline/DBSA to sepiolite is 2:1. With further increases in the weight percentage of aniline/DBSA, the conductivity of the PANI nanoclay changes little. The conductivity of the PANI nanoclay was found to increase and reached the level of PANI with the ratio increase of aniline/DBSA to sepiolite. Hence, it may be said that particles of sepiolite are well coated with PANI. For low weight percentages of aniline/DBSA, the coating of PANI on all sepiolite particles may not be proper because the relative proportion of aniline to sepiolite is decreased. Therefore, the formation of a conducting path through the aggregation of conducting particles is disturbed, leading to the decrease in conductivity.

The morphologies of the core–shell PANI-nanoclay particles were observed in the SEM images (Fig. 1b–d). The particles prepared in different contents of sepiolite are similar in general forms. This suggests that the ratio of sepiolite to aniline/DBSA has few effects on the general morphologies of the particles. However, with the increase of the aniline/DBSA ratio, the diameter of the PANI-nanoclay rod grows quickly, as shown in Fig. 1c.

The sepiolite fibrillar single crystals have a diameter of about 10 nm, as shown in Fig. 1a, and their lengths were different due to processing conditions. All the sepiolite needles were well encapsulated with thick PANI shells, and the resultant core–shell particles keep the needle-like

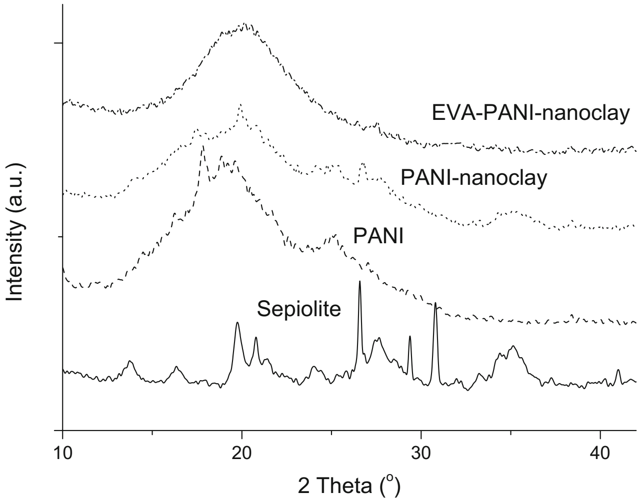

Fig. 3 X-ray diffraction patterns of sepiolite and PANI in different states

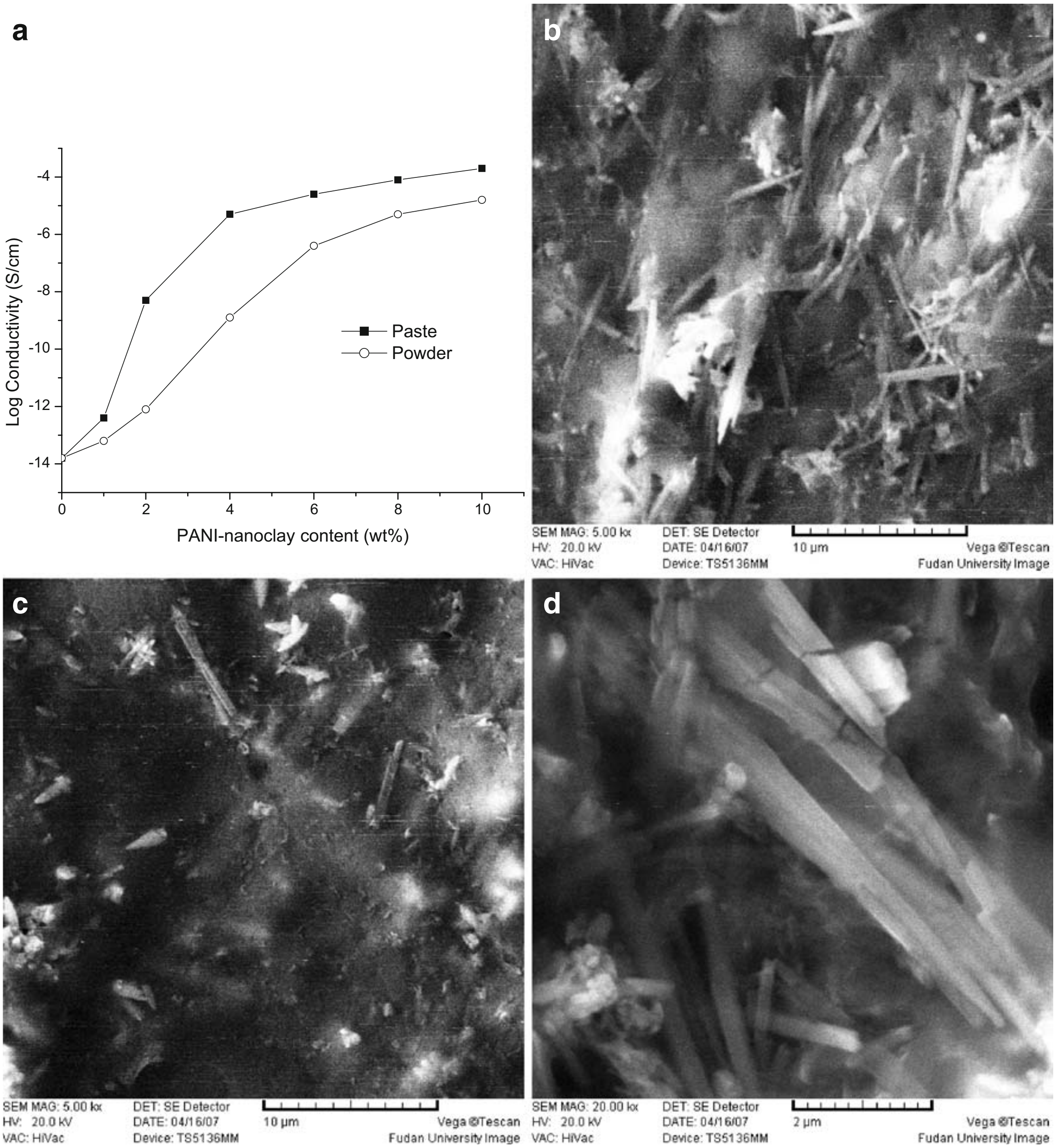

Fig. 4 Electrical conductivity and morphologies of EVA/PANI nanoclay as a function of PANI nanoclay content in both powder and paste forms. **a** Electrical conductivity; **b** SEM images of PANI nanoclay dispersed in EVA matrix via paste; **c** SEM images of PANI nanoclay dispersed in EVA matrix via powder; **d** magnified image of **c**

structure. However, comparing the diameter of core–shell particles with that of the initial sepiolite, one would find that the average diameter has increased several times during PANI polymerization. With the initial aggregations of sepiolite needles in Fig. 1a, it can be deduced that this increment in diameter also resulted from the conglutination of the sepiolite fibrillar single crystals through their surface PANI shells.

From high-magnified PANI-nanoclay particles in Fig. 1d, rough PANI was observed to precipitate on the surface of sepiolite. The X-ray diffraction patterns show the crystalline structure of sepiolite and neat PANI in Fig. 3. After PANI polymerized onto the surface of sepiolite, it also assembled some orientation from sepiolite as the peaks at about 26.5 and 35 °C clearly indicate this kind of structure duplication.

Based on the above results, in the following composites with EVA, the PANI-coated sepiolite used was prepared by maintaining the aniline/DBSA-to-sepiolite weight ratio at 2:1, and the product is designated as PANI nanoclay. As EVA latex has high affinity for nanoparticles from emulsion disperser and good miscibility with PANI due to the poly (vinyl acetate) components, with another advantage of low pH value, which would not dedope PANI during blending, the conductive composites would be anticipated to have a low percolation threshold.

In an effort to investigate the parameters that influence the dispersion of particles and electrical properties of the EVA/PANI-nanoclay blends, samples were prepared by blending EVA latex with either powder or paste PANI nanoclay. It is found that powder PANI nanoclay cannot be well dispersed in the EVA latex even after ultrasonic mixing. The volume resistivity measurements of such blends (Fig. 4a) containing 4 wt.% powder PANI nanoclay show that they are almost insulators (conductivity$<10^{-10}$ S/cm), in contrast with the blends with the same amounts of paste PANI nanoclay at about 10^{-8} S/cm. The mixture of EVA latex with PANI nanoclay (paste) is a green colloid with an excellent dispersion, as the latex can be preserved for 6 months without any signs of deterioration. The X-ray diffraction patterns of EVA–PANI nanoclay (paste) shown in Fig. 3 demonstrate the well dispersion of PANI nanoclay into EVA; the disappearance of peaks at 25, 26.5, and 35 °C indicates that PANI has partially dissolved into EVA matrix.

The different morphologies are compared in Fig. 4. For the 4 wt.% powder blend (Fig. 4c), the poor dispersion of PANI nanoclay leads to the creation of agglomerates (Fig. 4d), which are bundles of PANI-nanoclay rods together mostly surrounded by the insulating matrix and unable to come into contact with each other. On the other hand, the use of paste PANI nanoclay promotes the dispersion of the conductive nanofiber in the matrix (Fig. 4b), resulting in the formation of a very fine network. Thus, the quality of PANI nanoclay dispersion is closely related to the final electrical properties of the blends. The formation of a PANI-nanoclay network in the EVA matrix leads to enhanced electrical properties.

In summary, we have developed a facile way to disperse nanoscaled PANI into polymer matrix through the method described in Scheme 1. By using one-dimensional nanoclay as template, PANI was successfully polymerized onto the nanoclay surface to form well dispersed conductive nanorod into aqueous medium. During the polymerization process, the PANI-nanoclay rod grows both in diameter and length, which also comes from the aggregations of sepiolite nanorods. Through blending with latex form polymers, nanoconductive composites were obtained with high colloidal stability due to the high affinity of PANI to water and emulsion disperser and good miscibility of EVA with PANI. During the drying process, water evaporated from the latex and pushed nanorods to connect with each other due to volume shrinkages. As a result, a well dispersed EVA–PANI-nanoclay conductive composite was obtained with a low percolation threshold and high conductivity. We could anticipate that this kind of method would both increase the conductivity of PANI-based materials and economize the cost of PANI manufacturing.

Conclusions

The well dispersed one-dimensional nanostructures were synthesized from PANI-coated sepiolite nanofibers via in situ oxidative polymerization after the surface modification of the sepiolite with ammonium and anilinium salts. With the increase of the aniline to sepiolite ratio, the conductivity of resultant PANI nanoclay can reach the same level of neat PANI. When blending with EVA latex, the paste form of PANI nanoclay shows a low percolation threshold for conductivity and high colloidal stability due to its well dispersion in EVA matrix.

Acknowledgements This research was supported by the National Natural Science Foundation of China (20704008), Specialized Research Fund for the Doctoral Program of Higher Education of China (20070246001), Key Project Science Foundation of Shanghai Municipal Commission of Education (06zz78), and the Juan de la Cierva Program, Ministry of Education and Science, Spain.

References

1. Kirkpatrick S (1973) Rev Mod Phys 45:574
2. Zallen R (1983) The physics of amorphous solids. Wiley, New York
3. Gangopadhyay R, De A (2000) Chem Mater 12:608–622
4. Banerjee P, Mandal BM (1995) Macromolecules 28:3940–3943
5. Chen Z, Brokken-Zijp JCM, Huinink HP, Loos J, de With G, Michels MAJ (2006) Macromolecules 39:6115–6124
6. Cui S, Canet R, Derre A, Couzi M, Delhaes P (2003) Carbon 41:797–809
7. Li N, Huang Y, Du F, He XB, Lin X, Gao HJ, Ma YF, Li FF, Chen YS, Eklund PC (2006) Nano Lett 6:1141–1145
8. Fukushima T, Kosaka A, Yamamoto Y, Aimiya T, Notazawa S, Takigawa T, Inabe T, Aida T (2006) Small 2:554–560
9. Tans SJ, Verschueren ARM, Dekker C (1998) Nature 393:49–52
10. Joo J, Park KT, Kim BH, Kim MS, Lee SY, Jeong CK, Lee JK, Park DH, Yi WK, Lee SH, Ryu KS (2003) Synth Met 135:7–9
11. Shi XY, Briseno AL, Sanedrin RJ, Zhou FM (2003) Macromolecules 36:4093–4098
12. Barthet C, Armes SP, Lascelles SF, Luk SY, Stanley HME (1998) Langmuir 14:2032–2041
13. Niu ZW, Yang ZH, Hu ZB, Lu YF, Han CC (2003) Adv Funct Mater 13:949–954
14. Schnitzler DC, Meruvia MS, Hummelgen IA, Zarbin AJG (2003) Chem Mater 15:4658–4665
15. Xu J, Li XL, Liu JF, Wang X, Peng Q, Li YD (2005) J Polym Sci A Polym Chem 43:2892–2900
16. Huang K, Zhang YJ, Long YZ, Yuan JH, Han DX, Wang ZJ, Niu L, Chen Z (2006) Chemistry 12:5314–5319
17. Lahav M, Weiss EA, Xu QB, Whitesides GM (2006) Nano Lett 6:2166–2171
18. Sainz R, Benito AM, Martinez MT, Galindo JF, Sotres J, Baro AM, Corraze B, Chauvet O, Maser WK (2005) Adv Mater 17:278–281

19. Guo HF, Zhu H, Lin HY, Zhang JQ (2008) Mater Lett 62:3919–3921
20. Wu TM, Lin YW (2006) Polymer 47:3576–3582
21. Yu YJ, Che B, Si ZH, Li L, Chen W, Xue G (2005) Synth Met 150:271–277
22. Zhu Y, Zhang JC, Zheng YM, Zhai J, Jiang L (2006) Chem J Chin Univ 27:196–198 (Chinese)
23. Cheng QL, Pavlinek V, He Y, Li CZ, Lengalova A, Saha P (2007) Eur Poly J 43:3780–3786
24. Jiang J, Li LC, Xu F (2007) Mater Sci Eng A Struct Mater Prop Microstruct Process 456:300–304
25. Liu YS, Liu P, Su ZX (2007) Synth Met 157:585–591
26. Jang J, Bae J, Choi M, Yoon SH (2005) Carbon 43:2730–2736
27. Do Nascimento GM, Corio P, Novickis RW, Temperini MLA, Dresselhaus MS (2005) J Polym Sci A Polym Chem 43:815–822
28. Blanchet GB, Fincher CR, Gao F (2003) Appl Phys Lett 82:1290–1292
29. Yu YJ, Si ZH, Chen SJ, Bian CQ, Chen W, Xue G (2006) Langmuir 22:3899–3905
30. Hu JW, Li MW, Zhang MQ, Xiao DS, Cheng GS, Rong MZ (2003) Macromol Rapid Commun 24:889–893
31. Goh SH, Chan HSO, Ong CH (1996) Polymer 37:2675–2679
32. Barra GMO, Leyva ME, Soares BG, Sens M (2002) Synth Met 130:239–245
33. Tang JS, Jing XB, Wang BC, Wang FS (1988) Synth Met 24:231–238